

## Supporting Information for

### Pt Single-atoms Supported on Nitrogen-doped Carbon Dots for Highly Efficient Photocatalytic Hydrogen Generation

Hui Luo,<sup>a, b</sup> Ying Liu,<sup>b</sup> Stoichko D. Dimitrov,<sup>b, c</sup> Ludmilla Steier,<sup>d</sup> Shaohui Guo,<sup>e</sup> Xuanhua Li,<sup>e</sup> Jingyu Feng,<sup>a</sup> Fei Xie,<sup>a, b</sup> Yuanxing Fang,<sup>f</sup> Andrei Sapelkin,<sup>b</sup> Xinchen Wang<sup>f</sup> and Maria-Magdalena Titirici<sup>a\*</sup>

\*Corresponding authors: [m.titirici@imperial.ac.uk](mailto:m.titirici@imperial.ac.uk)

#### 1. Reagents

Chitosan (medium molecular weight), Chloroplatinic acid hydrate (99.995% trace metals basis), ammonium hydroxide (25 wt%), hydrogen peroxide (30 wt%), 1% 3-glycidoxypropyldimethoxymethylsilane, sulfuric acid (98 wt%), titanium diisopropoxide bis (acetylacetonate), platinum(IV) oxide (PtO<sub>2</sub>) and platinum(II) chloride (PtCl<sub>2</sub>), sodium sulfide, sodium sulphite, X-100 Triton and phosphate buffer solution were purchased from Sigma-Aldrich. Fluorine-doped tin oxide (FTO) coated glass was purchased from Solaronix. Filter paper was bought from VWR. All the chemicals are used as-received without further purification.

#### 2. Experimental Procedures

##### The synthesis of NCDs

NCDs were prepared by a one-step solvothermal carbonization as we reported before.<sup>[1]</sup> Typically, 1.4 g chitosan was dispersed in ethanol (4% w/v) and then the mixture was transferred into a 50 mL Teflon-sealed autoclave and maintained at 200°C for 12 hours. The obtained dark brown liquid phase was centrifuged at 20,000 rpm for 10 min to separate the liquid containing fluorescent NCDs from the solid black carbonaceous precipitate. The liquid phase containing NCDs was then filtered using standard syringe filters (0.2 µm pore size).

### **The photo-deposition of Platinum on NCDs surface**

The protocol for Pt doping on NCD surface was modified from the preparation method published by Sun *et al.*<sup>[2]</sup> Briefly, the NCDs solution with targeted optical density was prepared, and  $\text{H}_2\text{PtCl}_6$  was added dropwise to the solution until the desired final molar concentration (0.3 mM) was obtained. The optically transparent mixture in a cylindrical quartz cell with flat front and back windows was irradiated in the deposition setup through a 420 nm cut-off filter for 5 min. The Pt-modified NCDs are named Pt-NCDs.

### **The preparation of nanocrystal cellulose (NCC) template**

The NCC suspensions were prepared via sulfuric acid hydrolysis, referring to the previously reported method.<sup>[3]</sup> Every 1 g filter paper was hydrolysed in 8.75 ml 64 wt% sulfuric acid. The reaction was allowed to take place at 45 °C in a water bath. After 50-min vigorous stirring, a light-yellow suspension was obtained. 10-fold distilled water was added to the suspension to quench the hydrolysis, then the suspension was settled overnight and the top clear layer was discarded to remove the free acid. The remained white suspension was centrifuged twice at 12000 rpm for 15 min. The top clear liquid was discarded and the same amount of distilled water was added to re-disperse the white deposits. After the second centrifugation, the re-dispersed suspension was sonicated for 30 min, or until the big chunks in the suspension mostly dispersed. Then a third centrifugation was carried out, after which the top layer became turbid. The top NCC suspension was then extracted and dialyzed against distilled water for around 4 days until the pH of the water became constant. A bluish colloidal NCC suspension with the concentration around 1 wt% would be obtained after sonication for 30 min. Finally, to get the 6 wt% NCC solution, colloidal NCC suspension was concentrated by evaporating at ambient conditions.

### **The hybridization of NCDs and Pt-NCDs with NCC-templated $\text{TiO}_2$ films**

The  $\text{TiO}_2$  mesoporous films were prepared by a sol-gel method.<sup>[4]</sup> For the preparation of sol-gel precursor, 1.138 mL (2.3mmol) titanium diisopropoxide bis(acetylacetonate) was added dropwise to 8.567 mL isopropanol under continuous stirring for 30 min to obtain a homogeneous solution. Then, 7.645 mL 6 wt% NCC aqueous solution was added and stirred for 1 hour until the mixture turned into light yellow gel-like solution. Finally, 3 drops of X-100 Triton were added to reduce the surface tension and the solution was further stirred for 1 hour prior to the film deposition. For film fabrication, the precursor solution was spin-coated on FTO glass, followed by slow calcination at 450 °C for 2 h by using 2 °C/min ramp with 1 h of

continuous heating step at 200 °C. After naturally cooling down, the films were immersed in NCDs or Pt-NCDs solution for 24 hours. The white colour TiO<sub>2</sub> electrode turned light brown indicating that NCDs were uniformly decorated on the TiO<sub>2</sub> surface. Finally, the electrode was washed with ethanol and 200 °C treated in 5% H<sub>2</sub>/N<sub>2</sub> flow.

### **3. Characterization**

The morphology of TiO<sub>2</sub> films were studied by scanning electron microscopy (SEM, FEI Inspect F), transmission electron microscopy (TEM, Jeol JEM 2010). HAADF-STEM images and EDX mapping was carried out with a probe aberration-corrected analytical electron microscope (JEOL ARM200F) in scanning TEM (STEM) mode with electron beam voltage set at 200 kV. Imaging conditions were: 12 cm condenser lens, 40 μm C12 aperture with 3 mm bright field aperture. The X-ray diffraction (XRD) patterns were performed using Panalytical Xpert Pro diffractometer with Cu-Kα radiation. UV-Vis absorption spectra of NCDs in ethanol were recorded using Perkin Elmer Lambda LS 35 UV-visible spectrometer, and UV-Vis of TiO<sub>2</sub> films were performed on a Perkin Elmer Lambda LS 950 UV-visible spectrometer equipped with an integrating sphere in transmission mode. The XPS of NCDs and Pt-NCDs were conducted on a ThermalFisher Nexsa using Al K<sub>α1</sub> (1486.74 eV) X-ray source radiation produced by a monochromatized X-Ray source at operating power of 300W (15 kV × 20 mA). Samples were drop-cast on conductive glass substrates and dried under N<sub>2</sub> flow.

#### **Synchrotron X-Ray Absorption Fine Spectroscopy**

Ex-situ Pt L<sub>3</sub> edge XAS measurements were conducted at beamline B18 in Diamond Light Source, with *ca.* 3 GeV electron energy operation condition in fluorescence mode. Pt foil with 25 μm thickness was used to calibrate the Si (111) double-crystal monochromator, and used for data collection as a Pt standard afterwards. Two additional reference compounds were also measured: platinum(IV) oxide (PtO<sub>2</sub>) and platinum(II) chloride (PtCl<sub>2</sub>). The XAS data was processed with Athena and Artemis software, and a total of 9 or 18 spectra were averaged for each sample to reduce the noise-to-signal ratio.

#### **Photocatalytic activity for H<sub>2</sub> evolution**

The photocatalytic H<sub>2</sub> evolution reaction (HER) was conducted in a gastight quartz cell under visible light irradiation ( 0.5 W/cm<sup>2</sup>, 300 W Xe arc lamp with 420 nm UV light cut-off filter) in an aqueous electrolyte solution containing hole scavenger (0.3 M Na<sub>2</sub>S and 0.3 M Na<sub>2</sub>SO<sub>3</sub> in 50 mL deionized water). The amount of photocatalysts used was determined from scratched off powder from the films by weighing 3 samples each and calculating the average (1.53 ± 0.21

mg for Pt-NCDs/TiO<sub>2</sub> and 1.39 ± 0.33 mg for Pt NPs/TiO<sub>2</sub>). During the photocatalytic reaction, a gas chromatography (Shimadzu GC-2014c) equipped with a thermal conductivity detector (TCD) was employed to quantify the H<sub>2</sub> produced with a time interval every half hour.<sup>[2]</sup>

#### Calculation of the H<sub>2</sub> generation rate and turnover frequency (TOF)

$$\text{H}_2 \text{ rate (Pt-NCDs/TiO}_2 \text{ (0.2 wt \%))} = \frac{n_{(\text{H}_2)}}{m_{(\text{Pt})} * \tau} = \frac{175.3 \times 10^{-3} \text{ mmol}}{0.2 \% \times 1.53 \text{ mg} \times h} = 57.3 \text{ mmol h}^{-1} \text{ mg}_{\text{Pt}}^{-1}$$

$$\text{H}_2 \text{ rate (Pt NPs/TiO}_2 \text{ (0.78 wt \%))} = \frac{n_{(\text{H}_2)}}{m_{(\text{Pt})} * \tau} = \frac{75.6 \times 10^{-3} \text{ mmol}}{0.78 \% \times 1.39 \text{ mg} \times h} = 7.0 \text{ mmol h}^{-1} \text{ mg}_{\text{Pt}}^{-1}$$

$$\text{TOF (Pt-NCDs/TiO}_2 \text{ (0.2 wt \%))} = \frac{n_{(\text{H}_2)}}{n_{(\text{Pt})} * \tau} = \frac{175.3 \times 10^{-6} \text{ mol}}{0.2 \% \times 0.00153 \text{ g}/195 \times h} = 11171 \text{ h}^{-1}$$

$$\text{TOF (Pt-NCDs/TiO}_2 \text{ (0.78 wt \%))} = \frac{n_{(\text{H}_2)}}{n_{(\text{Pt})} * \tau} = \frac{75.6 \times 10^{-6} \text{ mol}}{0.78 \% \times 0.00139 \text{ g}/195 \times h} = 1359 \text{ h}^{-1}$$

Here  $\tau$  is the unit time of reaction.

#### 4. EXAFS fitting process

In Artemis fitting process, two single scattering paths of corresponding neighbours: Pt-N and Pt-C are calculated in FEFF. Models used in FEFF calculation for these paths have the same coordinates to keep the fit consistent for three paths. Many-body amplitude-reduction factor was also set as constant value 0.962 based on Pt foil reference. Three parameters were used in the fit: coordination number  $N$ , radial distance  $R$  and mean square relative displacements  $\sigma^2$ . In **Figure S6b**,  $\chi(k)$  data are shown fitted in  $k$ -space within the window-range of 3-12 Å<sup>-1</sup>, to minimise the goodness of fit parameter ( $\chi^2$ ) between the experimental data and a theoretical model.<sup>[6]</sup> The fitting results are listed in the **Table S1**. The Pt-C path, among all, has the best fit result according to the lowest  $\chi^2$  value. C and N were hard to be distinguished in EXAFS due to their similar back scattering amplitude and potential<sup>[7]</sup>. However, we can rank the Pt-X bonding preference by fixing all other factors within the fit process. The FT-EXAFS of two fit results in **Figure S6a** also confirms it through visual observation.

#### 5. Supporting Figures

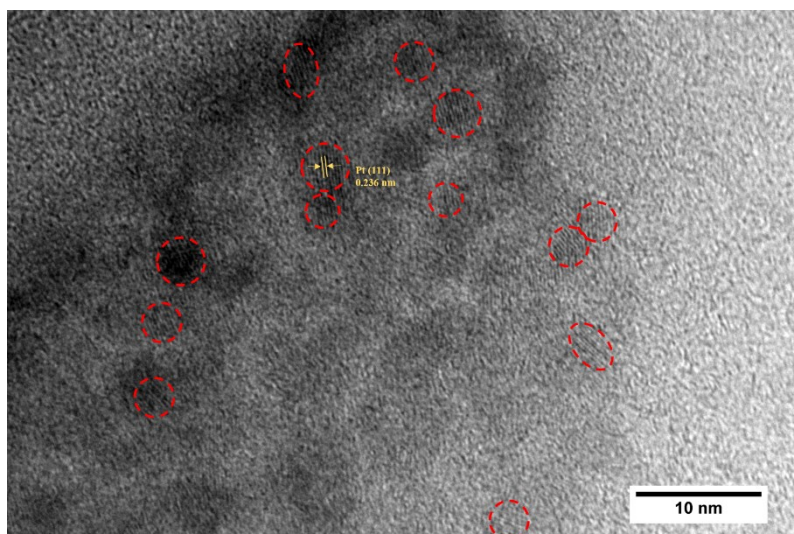


Figure S1. TEM image of Pt nanocrystalline structures on NCDs with 10 min deposition time.

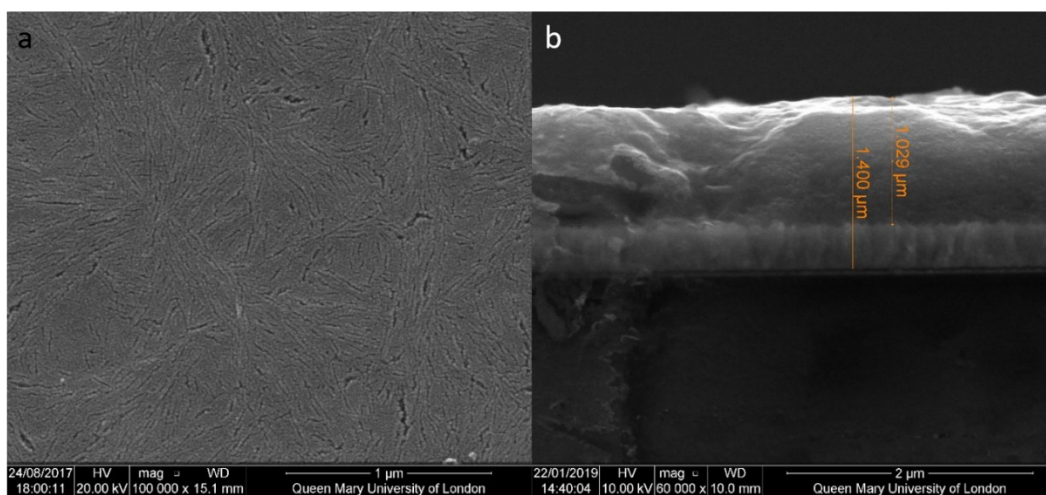


Figure S2. SEM top-view (a) and cross-section (b) images of Pt-NCDs/TiO<sub>2</sub> film.

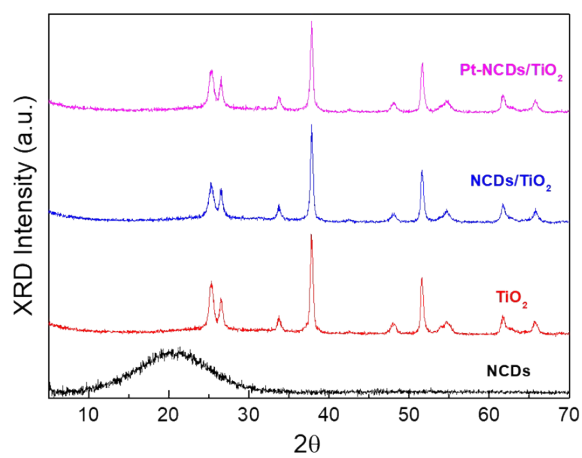


Figure S3. XRD patterns of NCD powder and TiO<sub>2</sub> films with different decorations.

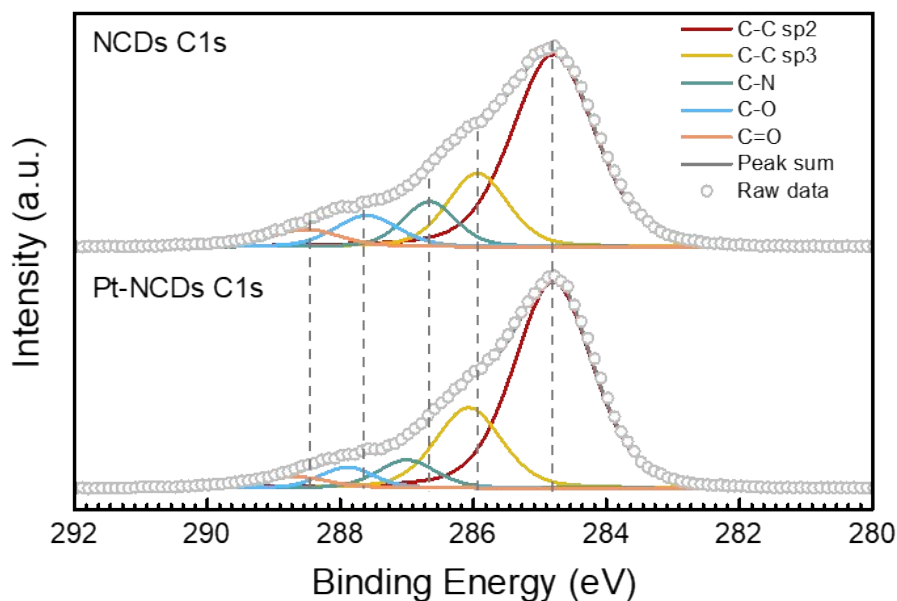


Figure S4 High-resolution XPS C 1s spectra of (Pt)-NCDs showing the binding energy shift due to the presence of Pt atoms.

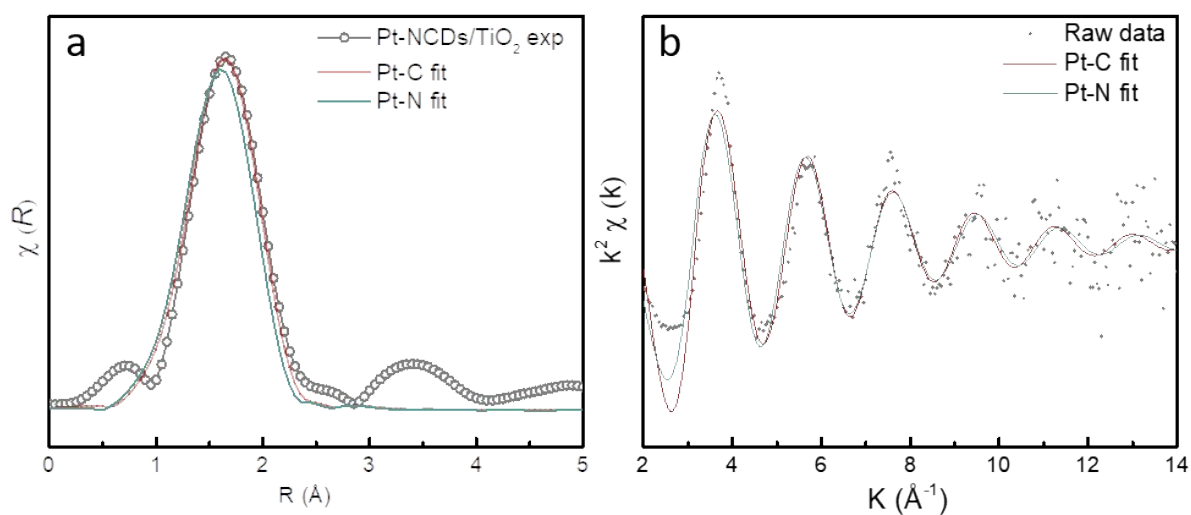
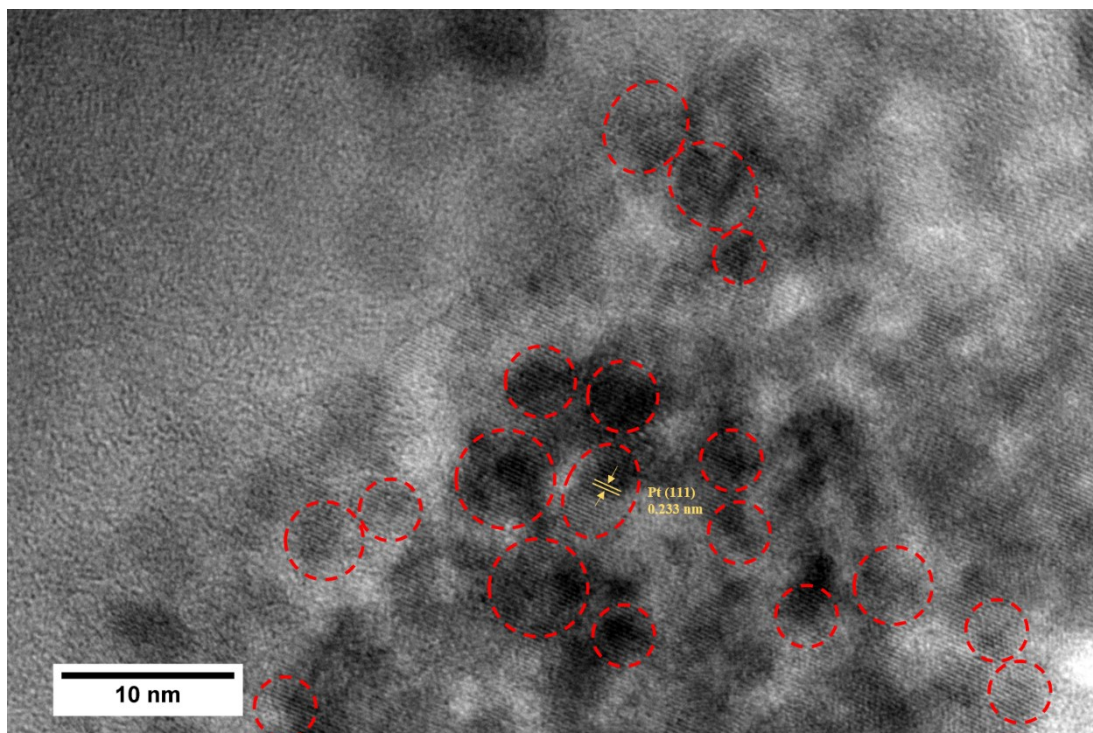


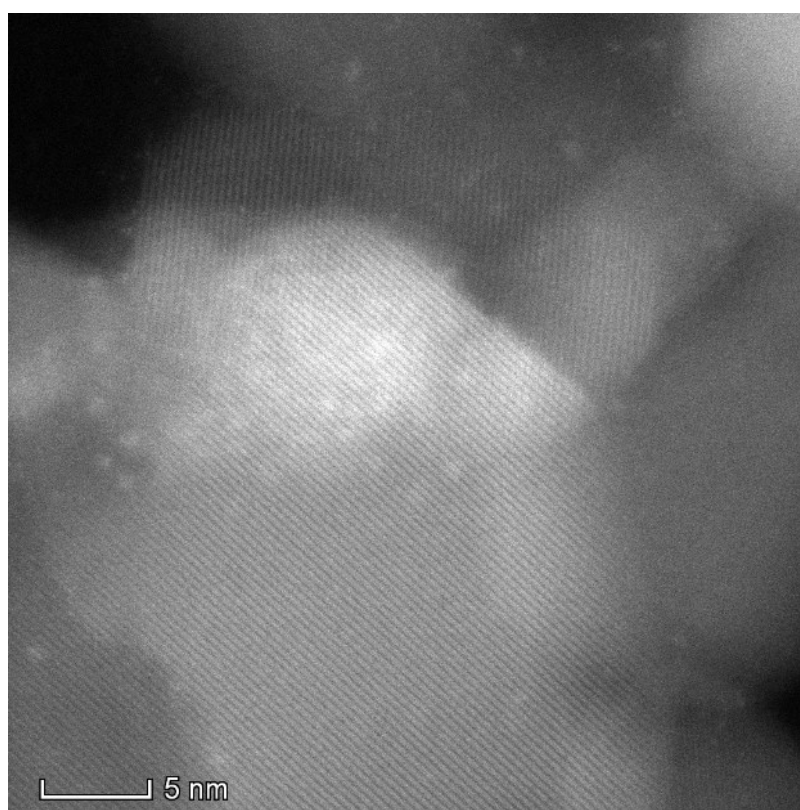
Figure S5 (a) FT-EXAFS curves between the experimental data and Pt-C, Pt-N fit. (b) Pt-C and Pt-N single scattering bond paths are used to fit Pt-NCDs/TiO<sub>2</sub> sample EXAFS  $\chi$  data in the  $k$ -range of 3 to 12.

Table S1. The Artemis EXAFS fit result of Pt-NCDs/TiO<sub>2</sub> sample

	Pt-C	Pt-N
N	4.71 ± 2.26	2.96 ± 1.68
R (Å)	2.05 ± 0.02	1.99 ± 0.02
$\sigma^2$	0.0055 ± 0.0045	0.0058 ± 0.0055
$\chi^2$	2716720	3466449



*Figure S6 UV light induced Pt nanoparticles formation.(irradiation time: 5 min)*



*Figure S7 Pt nanoparticles anchored on TiO<sub>2</sub> without NCDs.*

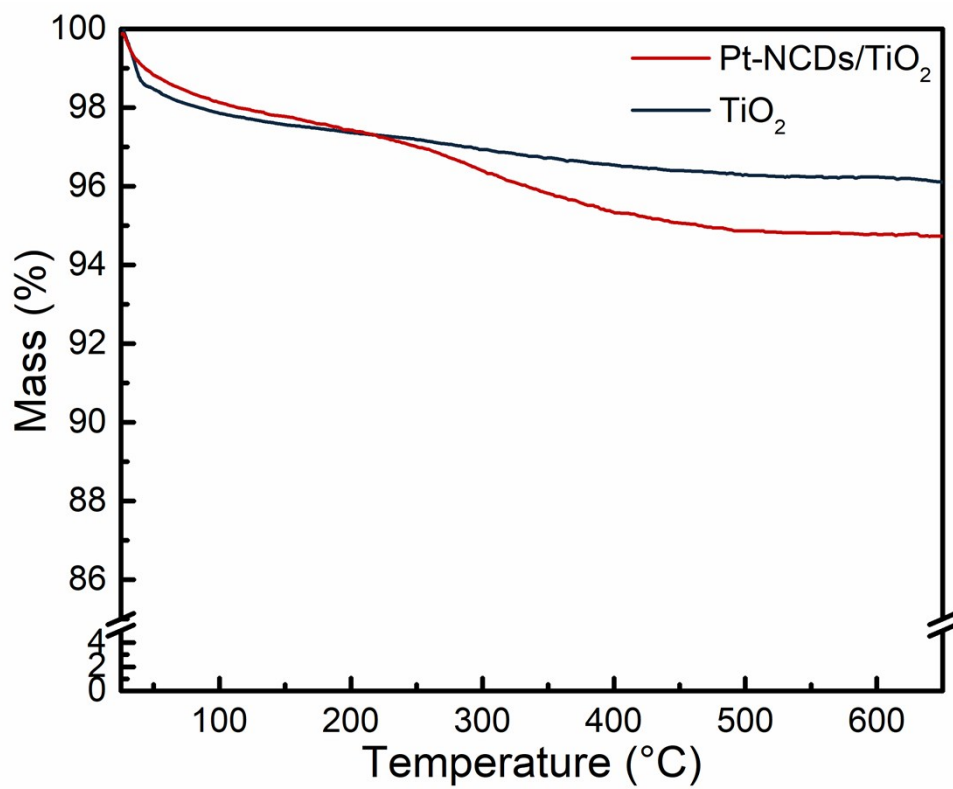


Figure S8 TGA spectra showing the mass loss in TiO<sub>2</sub> and Pt-NCDs/TiO<sub>2</sub> samples. The Pt-NCDs loading were calculated based on the mass loss percentage.

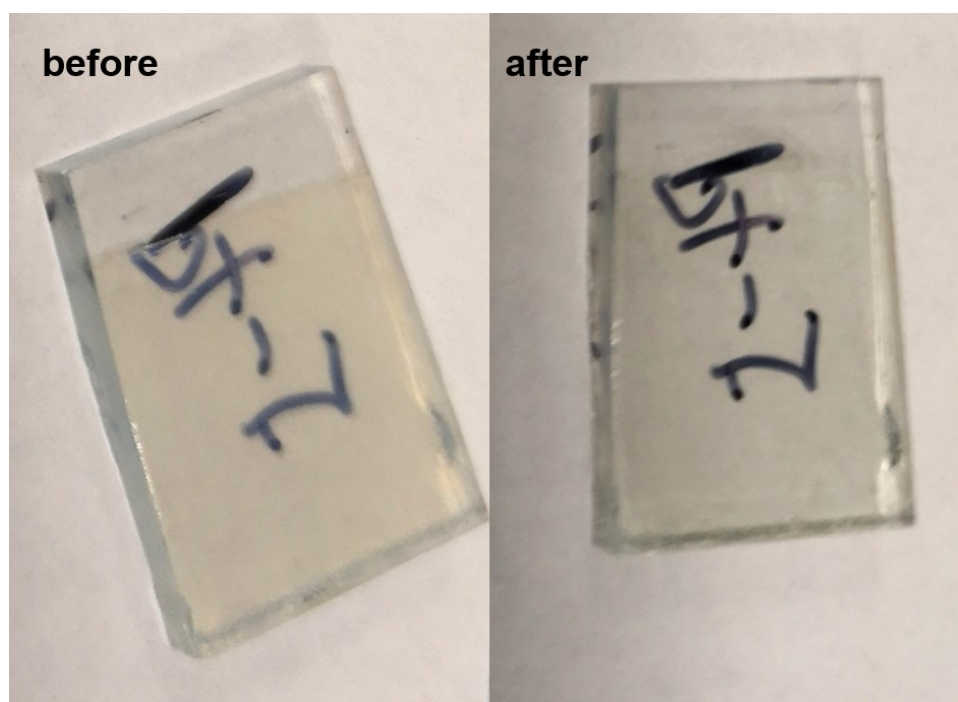


Figure S9 one Pt-NCDs/TiO<sub>2</sub> film before/after catalyst layer scratching off.



Table S2. Summary of hydrogen production rates and turnover frequencies for metal based cocatalysts (cal: calculated based on the efficiency reported in the literature; report: reported by the authors)

<b>Cocatalyst/photocatalyst (SACs: single-atom catalysts)</b>	<b>light source</b>	<b>sacrificial agent</b>	<b>H<sub>2</sub> production rate (mmol h<sup>-1</sup> mg<sub>(metal)</sub><sup>-1</sup>)</b>	<b>TOF (h<sup>-1</sup>)</b>	<b>ref</b>
0.2 wt% Pt SACs/TiO <sub>2</sub>		30% v/v methanol aqueous solution	4.24 (cal)	~826.8 (report)	[8]
Pt SACs/g-C <sub>3</sub> N <sub>4</sub>	300 W Xe lamp	10 vol% triethanolamine aqueous solution	~4.2 (cal)	775 (cal)	[7]
Co SACs-NG/CdS	300 W Xe lamp equipped with a 420 nm UV cut-off filter	1M aqueous (NH <sub>4</sub> ) <sub>2</sub> SO <sub>3</sub> solution	5.528 (cal)	325.5 (cal)	[9]
1.0 wt% Pt/TiO <sub>2</sub>	300 W Xe lamp equipped with an AM 1.5 G filter	29 v/v % ethanol aqueous solution	7.41 (report)		[10]
3.5 wt% Co SACs-NG/TiO <sub>2</sub>	300 W Xe lamp equipped with an AM 1.5 G filter	29 v/v % ethanol aqueous solution	6.77 (report)		[10]
0.6 wt% Pt SACs/TiO <sub>2</sub> -A	300 W Xe lamp	20 v/v % methanol aqueous solution	1.408 (cal)	274 (cal)	[11]
1.15 wt% Pt SACs/CdS@CDs	300 W Xe lamp	0.35M Na <sub>2</sub> SO <sub>3</sub> and 0.25M Na <sub>2</sub> S	3.96 (cal)	771.5 (cal)	[12]
0.6 wt% Pt SACs/TiO <sub>2</sub> -(001)	300 W Xe lamp	10 v/v % methanol aqueous solution	3.65 (cal)	711.75 (cal)	[13]
0.188 wt% NYTiO <sub>2</sub> -Pt-0.5	300 W Xe lamp	37.5 v/v % methanol aqueous solution	11.1 (cal)	2165.7 (cal)	[14]
HNTM-Ir (1.05 wt%)/Pt (2.54 wt%)	300 W Xe lamp equipped with a 400 nm cut off filter	TEOA	0.006 (cal)		[15]
0.5 wt% Ni SACs-NG/CdS	300 W Xe lamp equipped with a 420 nm cut off filter	1 M (NH <sub>4</sub> ) <sub>2</sub> SO <sub>3</sub> aqueous solution	20241 (cal)	2376000 (report)	[16]
0.18 wt% g-C <sub>3</sub> N <sub>4</sub> -Pt <sup>2+</sup>	300 W Xe lamp equipped with a 400 nm cut off filter	TEOA	0.33 (cal)		[17]
Pt (0.6 wt%)-Au (0.8 wt%)/C <sub>3</sub> N <sub>4</sub>	300 W Xe lamp	no sacrificial agent	0.02		[18]
0.2 wt% Pt SACs-	300 W Xe lamp equipped with a	0.3 M Na <sub>2</sub> SO <sub>3</sub> and 0.3M Na <sub>2</sub> S	57.3	11171	this work

NCDs/TiO <sub>2</sub>	420 nm UV cut-off filter				
0.78 wt% Pt NPs/TiO <sub>2</sub>	300 W Xe lamp equipped with a 420 nm UV cut-off filter	0.3 M Na <sub>2</sub> SO <sub>3</sub> and 0.3M Na <sub>2</sub> S	6.3	1235	this work

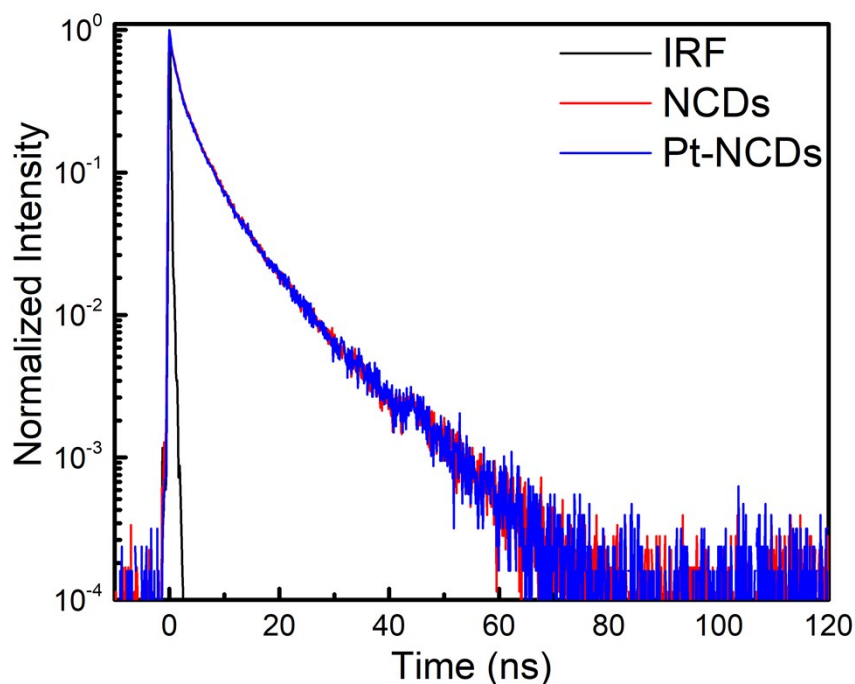


Figure S10 PL decay profile of aqueous NCDs and Pt-NCDs solutions.

## 6. Reference

- [1] D.-W. Zhang, N. Papaioannou, N. M. David, H. Luo, H. Gao, L. C. Tanase, T. Degou  e, P. Samor  , A. Sapelkin, O. Fenwick, et al., *Mater. Horizons* **2018**, *5*, 423–428.
- [2] J. Xu, S. Sahu, L. Cao, C. E. Bunker, P. Ge, L. Yamin, K. a S. Fernando, P. Wang, E. a Guliants, M. J. Meziani, et al., *Langmuir* **2012**, *28*, 16141–16147.
- [3] K. E. Shopsowitz, W. Y. Hamad, M. J. MacLachlan, *Angew. Chemie - Int. Ed.* **2011**, *50*, 10991–10995.
- [4] A. Ivanova, M. C. Fravventura, D. Fattakhova-Rohlfing, J. Rathousk  y, L. Movsesyan, P. Ganter, T. J. Savenije, T. Bein, *Chem. Mater.* **2015**, *27*, 6205–6212.
- [5] S. Guo, X. Li, X. Ren, L. Yang, J. Zhu, B. Wei, *Adv. Funct. Mater.* **2018**, *28*, 1–13.
- [6] M. Newville, *J. Synchrotron Radiat.* **2001**, *8*, 322–324.
- [7] X. Li, W. Bi, L. Zhang, S. Tao, W. Chu, Q. Zhang, Y. Luo, C. Wu, Y. Xie, *Adv. Mater.* **2016**, *28*, 2427–2431.
- [8] J. Xing, J. F. Chen, Y. H. Li, W. T. Yuan, Y. Zhou, L. R. Zheng, H. F. Wang, P. Hu, Y. Wang, H. J. Zhao, et al., *Chem. - A Eur. J.* **2014**, *20*, 2138–2144.

- [9] Q. Zhao, W. Yao, C. Huang, Q. Wu, Q. Xu, *ACS Appl. Mater. Interfaces* **2017**, *9*, 42734–42741.
- [10] L. Yi, F. Lan, J. Li, C. Zhao, *ACS Sustain. Chem. Eng.* **2018**, *6*, 12766–12775.
- [11] Y. Sui, S. Liu, T. Li, Q. Liu, T. Jiang, Y. Guo, J. L. Luo, *J. Catal.* **2017**, *353*, 250–255.
- [12] S. Qiu, Y. Shen, G. Wei, S. Yao, W. Xi, M. Shu, R. Si, M. Zhang, J. Zhu, C. An, *Appl. Catal. B Environ.* **2019**, *259*, 118036.
- [13] T. Wei, Y. Zhu, Y. Wu, X. An, L. M. Liu, *Langmuir* **2019**, *35*, 391–397.
- [14] J. Jin, C. Wang, X. N. Ren, S. Z. Huang, M. Wu, L. H. Chen, T. Hasan, B. J. Wang, Y. Li, B. L. Su, *Nano Energy* **2017**, *38*, 118–126.
- [15] T. He, S. Chen, B. Ni, Y. Gong, Z. Wu, L. Song, L. Gu, W. Hu, X. Wang, *Angew. Chemie - Int. Ed.* **2018**, *57*, 3493–3498.
- [16] Q. Zhao, J. Sun, S. Li, C. Huang, W. Yao, W. Chen, T. Zeng, Q. Wu, Q. Xu, *ACS Catal.* **2018**, *8*, 11863–11874.
- [17] Y. Li, Z. Wang, T. Xia, H. Ju, K. Zhang, R. Long, Q. Xu, C. Wang, L. Song, J. Zhu, et al., *Adv. Mater.* **2016**, 6959–6965.
- [18] H. Su, M. Liu, W. Cheng, X. Zhao, F. Hu, Q. Liu, *J. Mater. Chem. A* **2019**, *7*, 11170–11176.